

Quasinormal modes of charged black holes in string theory

Fu-Wen Shu^{1,3}, You-Gen Shen^{1,2} *

¹Shanghai Astronomical Observatory, Chinese Academy of Sciences, Shanghai 200030, People's Republic of China ,

² National Astronomical Observatories, Chinese Academy of Sciences, Beijing 100012, People's Republic of China ,

³Graduate School of Chinese Academy of Sciences, Beijing 100039, People's Republic of China.

Abstract

Both scalar and Dirac quasinormal modes in Garfinkle-Horowitz-Strominger black hole space-time are studied by using the WKB approximation and the Pöschl-Teller approximation. For scalar field, we find that the QNMs with higher dilatons decay more rapidly than that with lower ones. However, this is not the case for mass m . Fields with higher mass will decay more slowly. The similar behaviors appear in the case of Dirac field. We also find that QNM frequencies evaluated by using WKB approximation and Pöschl-Teller approximation have a good agreement with each other when mode number n is small.

PACS: number(s): 04.70.Dy, 04.70.Bw, 97.60.Lf

I INTRODUCTION

The stability of a black hole has been discussed for many years. The pioneering work on this problem was carried by Regge and Wheeler[1, 2], who studied the linear perturbation of Schwarzschild black hole. Vishveshwara[3] and Chandrasekhar[4] furthered this work by bringing forward quasinormal modes(QNMs). Being its importance both in the analysis of the stability of the black holes and in the search for black holes and its gravitational radiation, the QNMs of black holes in the framework of general relativity have been studied widely.

QNMs of black holes are defined as proper solutions of the perturbation equations belonging to certain complex characteristic frequencies which satisfy the boundary conditions appropriate for purely ingoing waves at the event horizon and purely outgoing waves at infinity[5]. Generally speaking, the evolution of field perturbation on a black hole consists roughly of three stages[6]. The first one is an initial wave dependent on the initial form of the original field perturbation. The second one involves the damped oscillations called QNMs, which frequencies and damping times are entirely fixed by the structure of the background spacetime and are independent of the initial perturbation. The last stage is a power-law tail behavior of the waves at very late time which is caused by backscattering of the gravitational field.

QNMs were firstly used to study the stability of a black hole. Then people used it to study the properties of black holes for the definite relations between the parameters of the black hole and its QNMs. Latest studies in asymptotically flat space have acquired a further attention because of the possible relation between the classical vibrations of black holes and various quantum aspects, which was proposed by relating the real part of the quasinormal frequencies to the Barbero-Immirzi parameter, a factor introduced by hand in order that loop quantum gravity reproduces correctly entropy of the black hole[7, 8, 9]. Moreover, QNMs also relate to superstring theory[10, 11]. This is known as the AdS/CFT correspondence, which argues that string theory in anti-de Sitter(AdS) space is equivalent to conformal field theory(CFT)in one less dimension.

*E-mail: ygshen@center.shao.ac.cn

We know that the Schwarzschild spacetime can describe an uncharged black hole in string theory very well (except in the region near the horizon) when the mass of the black hole is larger than the Plank mass. However, this is not the case for a charged black hole in string theory. Gibbons and Maeda[12] first obtained its solution in this case, latter Garfinkle, Horowitz and Strominger[13] find an another kind of solution, which is known as Garfinkle-Horowitz-Strominger solution. It has been showed that there exist many essential differences between the Garfinkle-Horowitz-Strominger black hole and the Reissner-Nordström black hole. This makes it necessary for us to study the QNMs of Garfinkle-Horowitz-Strominger dilaton black hole, although the similar work of Reissner-Nordström de Sitter black hole has been done by Ref.[14]. The main purpose of this paper is to study the QNMs of Garfinkle-Horowitz-Strominger dilaton black holes by evaluating the quasinormal mode frequencies both of scalar and Dirac fields.

Many methods are available for calculating the quasinormal mode frequencies. Most of them are numerical in nature. However, there are two methods often used, i.e., WKB potential approximation, which was devised and developed in[15, 16], and Pöschl-Teller(PT) potential approximation, which was first proposed by Pöschl and Teller[17]. Both methods have their own merits. WKB approximation is accurate for the low-lying modes[18], while the Pöschl-Teller approximation is simpler than the first one and accurate enough for our purpose. Therefore, we utilize the first method to calculate the frequencies of the scalar field, but use the second method to calculate the frequencies of the massive Dirac field. Moreover, we use these two methods to calculate the massless Dirac field so that we can check the consistency between these two kinds of methods.

The paper is organized as follows: In the next section we study the scalar QNMs in Garfinkle-Horowitz-Strominger dilaton black hole, and evaluate their quasinormal mode frequencies. In Sec.III, we discuss the Dirac QNMs and calculate their characteristic frequencies. Some conclusions are drawn in the last section.

II SCALAR QUASINORMAL MODES IN THE GARFINKLE-HOROWITZ-STROMINGER BLACK HOLE

We consider the QNMs in the Garfinkle-Horowitz-Strominger black hole described by the metric[13, 19]

$$ds^2 = -e^{2U} dt^2 + e^{-2U} dr^2 + R^2 (d\theta^2 + \sin^2\theta d\varphi^2), \quad (1)$$

$$e^{-2\phi} = e^{-2\phi_0} \left(1 - \frac{a}{r}\right), \quad (2)$$

$$F = Q \sin\theta d\theta \wedge d\varphi, \quad (3)$$

with

$$e^{2U} = 1 - \frac{2M}{r}, \quad (4)$$

$$R = \sqrt{r(r-a)}, \quad (5)$$

where M is the mass of the black hole, Q is magnetic charge, ϕ and F are scalar and magnetic field, respectively. The parameter a is defined by

$$a = \frac{Q^2}{2M} e^{-2\phi_0}, \quad (6)$$

and ϕ_0 is an arbitrary constant.

The best way to deal with the QNMs for the scalar field is to solve equations[13] deduced from the action. However, it is very difficult, if possible, to solve these equations because we must find general solutions rather than static, spherically symmetric solutions which obtained in Ref.[13] when we discuss scalar QNMs in Garfinkle-Horowitz-Strominger black hole. Under this consideration, we use another effective way to solve this question, the way has been used to discuss the entropy in Garfinkle-Horowitz-Strominger black hole in Ref.[19].

The scalar field with mass m satisfies the wave equation

$$(\square - m^2) \tilde{\Phi} = 0. \quad (7)$$

If we introduce a tortoise coordinate

$$dr_* = e^{-2U} dr, \quad (8)$$

and define

$$\tilde{\phi} = \tilde{\Phi} e^{-i\omega t}, \quad (9)$$

Then the wave equation can be written as

$$\frac{d^2 \tilde{\phi}}{dr_*^2} + (\omega^2 - V) \tilde{\phi} = 0. \quad (10)$$

where

$$V = \left(1 - \frac{2M}{r}\right) \left[\frac{M(2r-a)}{r^3(r-a)} - \left(1 - \frac{2M}{r}\right) \cdot \frac{a^2}{4r^2(r-a)^2} + \frac{l(l+1)}{r(r-a)} + m^2 \right]. \quad (11)$$

It is an extremal black hole for Garfinkle-Horowitz-Strominger black hole when $a = 2M$, since there exists a curvature singularity at $r = a$ as showed in Eqs.(1-5). In this case, many new unknown properties occur and thus further work is needed. In this article, we only calculate the quasinormal mode frequencies when $a \neq 2M$. It is obvious that the effective potential satisfies

$$\begin{aligned} V &\rightarrow e^{\frac{r_*}{2M}}, & \text{as } r_* &\rightarrow -\infty, \\ V &\rightarrow m^2, & \text{as } r_* &\rightarrow +\infty. \end{aligned}$$

As m is increased, the peak value of the effective potential will be smaller than the asymptotic value m^2 . Reference [20] pointed out that there will be no quasinormal modes if the peak of the potential is lower than the asymptotic value m^2 , i.e., there exists a maximum value above which quasinormal modes can not occur. Therefore, one can estimate its value m_{max} by using the relation

$$V(r_{max}, m_{max}, l, a) = m_{max}^2. \quad (12)$$

The results are tabulated in Table I. Here we have used the mass M of the black hole as a unit of mass.

l	$a = 0$	$a = 0.5$	$a = 1$	$a = 1.5$
1	0.3972	0.4250	0.4630	0.5231
2	0.6378	0.6834	0.7463	0.8472
3	0.8841	0.9474	1.0351	1.1766
4	1.1320	1.2132	1.3258	1.5077
5	1.3807	1.4798	1.6172	1.8396

Table I: Maximum values of the mass m of the scalar field above which QNMs can not occur.

From the discussion above, we see that we must let m smaller than m_{max} when we calculate the quasinormal mode frequencies. One can obtain the complex quasinormal mode frequencies ω by using WKB approximation. The formula, carried to third order beyond the eikonal approximation, is given by[16]

$$\begin{aligned} \omega_n^2 &= \left[V_0 + (-2V_0'')^{\frac{1}{2}} \Lambda \right] - \\ & i \left(n + \frac{1}{2} \right) (-2V_0'')^{\frac{1}{2}} (1 + \Omega), \end{aligned} \quad (13)$$

where

$$\Lambda = \frac{1}{(-2V_0'')^{1/2}} \left\{ \frac{1}{8} \left(\frac{V_0^{(4)}}{V_0''} \right) \left(\frac{1}{4} + \alpha^2 \right) - \frac{1}{288} \left(\frac{V_0'''}{V_0''} \right)^2 (7 + 60\alpha^2) \right\}, \quad (14)$$

Table II: Quasinormal mode frequencies for scalar field

m	l	n	a = 0	a = 0.5	a = 1	a = 1.5
0	1	0	0.2911-0.0980i	0.3202-0.1007i	0.3620-0.1038i	0.4330-0.1067i
		2	0.4832-0.0968i	0.5305-0.0996i	0.5985-0.1029i	0.7143-0.1060i
	5	1	0.4632-0.2958i	0.5126-0.3037i	0.5836-0.3128i	0.7046-0.3208i
		0	1.0596-0.0963i	1.1627-0.0992i	1.3112-0.1026i	1.5642-0.1058i
		1	1.0500-0.2902i	1.1541-0.2987i	1.3039-0.3087i	1.5593-0.3179i
		2	1.0320-0.4870i	1.1380-0.5009i	1.2903-0.5170i	1.5501-0.5318i
		3	1.0075-0.6874i	1.1159-0.7064i	1.2716-0.7283i	1.5374-0.7480i
		4	0.9779-0.8913i	1.0894-0.9152i	1.2491-0.9426i	1.5224-0.9667i
0.2	1	0	0.3091-0.0868i	0.3358-0.0915i	0.3748-0.0968i	0.4420-0.1021i
		2	0.4959-0.0924i	0.5414-0.0961i	0.6073-0.1002i	0.7203-0.1042i
	5	1	0.4695-0.2865i	0.5185-0.2959i	0.5886-0.3066i	0.7084-0.3166i
		0	1.0658-0.0954i	1.1680-0.0985i	1.3154-0.1020i	1.5671-0.1054i
		1	1.0554-0.2875i	1.1588-0.2966i	1.3078-0.3070i	1.5620-0.3168i
		2	1.0362-0.4831i	1.1417-0.4977i	1.2934-0.5145i	1.5523-0.5301i
		3	1.0101-0.6831i	1.1184-0.7028i	1.2738-0.7254i	1.5391-0.7460i
		4	0.9791-0.8871i	1.0906-0.9116i	1.2503-0.9396i	1.5234-0.9646i
0.3972	1	0	0.3612-0.0511i	0.3826-0.0607i	0.4133-0.0731i	0.4692-0.0867i
0.4	2	0	0.5347-0.0787i	0.5746-0.0848i	0.6340-0.0917i	0.7387-0.0987i
		1	0.4867-0.2582i	0.5347-0.2722i	0.6031-0.2879i	0.7195-0.3038i
	5	0	1.0844-0.0925i	1.1839-0.0961i	1.3281-0.1002i	1.5758-0.1042i
		1	1.0718-0.2795i	1.1729-0.2900i	1.3192-0.3020i	1.5699-0.3136i
		2	1.0486-0.4716i	1.1527-0.4882i	1.3025-0.5071i	1.5589-0.5252i
		3	1.0178-0.6701i	1.1256-0.6918i	1.2801-0.7168i	1.5439-0.7401i
		4	0.9825-0.8747i	1.0943-0.9009i	1.2539-0.9309i	1.5265-0.9583i

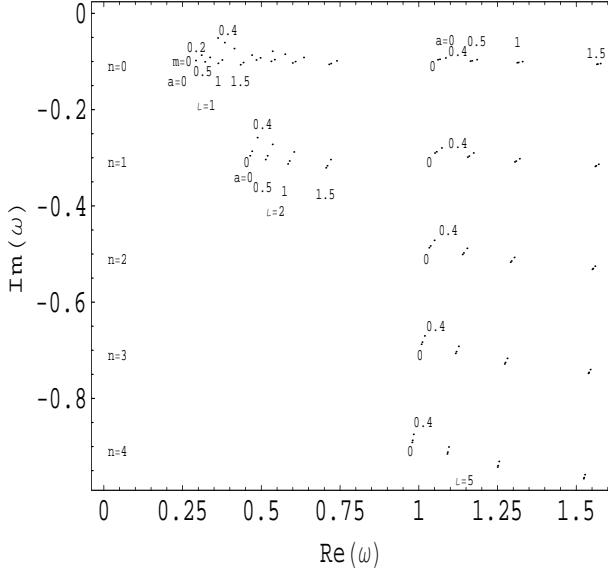


Figure 1: Scalar quasinormal mode frequencies

$$\begin{aligned}
\Omega = & \frac{1}{(-2V_0'')} \cdot \left\{ \frac{5}{6912} \left(\frac{V_0'''}{V_0''} \right)^4 (77 + 188\alpha^2) - \frac{1}{384} \left(\frac{V_0'''^2 V_0^{(4)}}{V_0''^3} \right) (51 + 100\alpha^2) \right. \\
& + \frac{1}{2304} \left(\frac{V_0^{(4)}}{V_0''} \right)^2 (67 + 68\alpha^2) + \frac{1}{288} \left(\frac{V_0'''' V_0^{(5)}}{V_0''^2} \right) (19 + 28\alpha^2) \\
& \left. - \frac{1}{288} \left(\frac{V_0^{(6)}}{V_0''} \right) (5 + 4\alpha^2) \right\}, \tag{15}
\end{aligned}$$

$$\alpha = n + 1/2, \quad \begin{cases} 0, 1, 2, \dots & R_e(\omega) > 0, \\ -1, -2, -3, \dots & R_e(\omega) < 0. \end{cases} \tag{16}$$

$$V_0^{(n)} = \left. \frac{d^n V}{dr_*^n} \right|_{r_* = r_*(r_0)}. \tag{17}$$

We can obtain the complex quasinormal mode frequencies by plugging the potential V in eq.(11) into the formula above. The values for $0 \leq l$ are listed in Table II. The values for negative n are related to those with positive n by reflection of the imaginary axis. Figure 1 is its corresponding figure.

III DIRAC QUASINORMAL MODES IN THE GARFINKLE-HOROWITZ-STROMINGER BLACK HOLE

The Dirac equation in a general background spacetime is[2]

$$[\gamma^a e_a^\mu (\partial_\mu + \Gamma_\mu) + m] \Psi = 0, \tag{18}$$

where e_a^μ is the inverse of the tetrad e_μ^a defined by the metric $g_{\mu\nu}$,

$$g_{\mu\nu} = \eta_{ab} e_\mu^a e_\nu^b, \tag{19}$$

and Γ_μ is the spin connection which is defined as $\Gamma_\mu = \frac{1}{8} [\gamma^a, \gamma^b] e_a^\nu e_{b\nu;\mu}$. If we define

$$\Psi = e^{-U/2} \begin{pmatrix} iG^\pm(r) \phi_{jm}^{(\pm)}(\theta, \varphi) / R \\ F^\pm(r) \phi_{jm}^{(\mp)}(\theta, \varphi) / R \end{pmatrix} e^{-i\omega t}, \tag{20}$$

and use the tortoise coordinate $dr_* = e^{-2U} dr$, the Dirac equation can be decoupled as

$$\frac{d}{dr_*} \begin{pmatrix} F \\ G \end{pmatrix} - e^U \begin{pmatrix} \kappa/R & m \\ m & -\kappa/R \end{pmatrix} \begin{pmatrix} F \\ G \end{pmatrix} = \begin{pmatrix} 0 & -\omega \\ \omega & 0 \end{pmatrix} \begin{pmatrix} F \\ G \end{pmatrix}, \tag{21}$$

where κ satisfies

$$\kappa = \begin{cases} j + \frac{1}{2}, & j = l + \frac{1}{2}; \\ -j - \frac{1}{2}, & j = l - \frac{1}{2}. \end{cases} \tag{22}$$

If we make a change of variables[5]

$$\begin{pmatrix} \tilde{F} \\ \tilde{G} \end{pmatrix} = \begin{pmatrix} \sin(\frac{\theta}{2}) & \cos(\frac{\theta}{2}) \\ \cos(\frac{\theta}{2}) & -\sin(\frac{\theta}{2}) \end{pmatrix} \begin{pmatrix} F \\ G \end{pmatrix}, \tag{23}$$

where $\theta = \tan^{-1}(\frac{mR}{\kappa})$. Eq.(21) becomes

$$\frac{d}{d\tilde{r}_*} \begin{pmatrix} \tilde{F} \\ \tilde{G} \end{pmatrix} + W \begin{pmatrix} -\tilde{F} \\ \tilde{G} \end{pmatrix} = \begin{pmatrix} \tilde{G} \\ -\tilde{F} \end{pmatrix}, \tag{24}$$

where we have made a coordinate transformation

$$\tilde{r}_* = r_* + \frac{1}{2\omega} \tan^{-1} \left(\frac{mR}{\kappa} \right), \quad (25)$$

and

$$W = \frac{e^U \left[(\kappa/R)^2 + m^2 \right]}{1 + \kappa m R' e^{2U} / [2\omega (\kappa^2 + m^2 R^2)]}. \quad (26)$$

Eq.(24) can also be written as

$$\frac{d^2 \tilde{F}}{d\tilde{r}_*^2} + (\omega^2 - V_1) \tilde{F} = 0, \quad (27)$$

$$\frac{d^2 \tilde{G}}{d\tilde{r}_*^2} + (\omega^2 - V_2) \tilde{G} = 0, \quad (28)$$

and

$$V_{1,2} = \pm \frac{dW}{d\tilde{r}_*} + W^2, \quad (29)$$

where $V_{1,2}$ are supersymmetric partners derived from the same superpotential. It is obvious that potentials related in this way possess the same characteristic frequencies for both \tilde{F} and \tilde{G} [21], which means that Dirac particles and antiparticles have the same quasinormal mode spectra in the Garfinkle-Horowitz-Strominger black hole spacetime. Therefore, it is reasonable to concentrate just on Eq.(27) in evaluating the quasinormal mode frequencies in the next sections.

A Quasinormal mode frequencies for the massless Dirac field

In this subsection, we shall evaluate the quasinormal mode frequencies of the massless Dirac field in the Garfinkle-Horowitz-Strominger black hole as $a \neq 2M$ by using WKB potential approximation and Pöschl-Teller potential approximation, so that we can compare the results with each other. Zhidenko[22] has proved that the quasinormal mode frequencies obtained by the Pöschl-Teller approximation and the sixth-order WKB approximation are in a very good agreement for the Schwarzschild de Sitter black hole.

We rewrite Eq.(27) as

$$\frac{d^2 \tilde{F}}{dr_*^2} + (\omega^2 - V) \tilde{F} = 0, \quad (30)$$

where

$$V = \frac{|\kappa| e^{2U}}{R^2} \left[|\kappa| \pm \left(R e^U U' - e^U R' \right) \right]. \quad (31)$$

Here we have written V_1 as V because we shall not consider V_2 , which will give the same spectrum of quasinormal mode frequencies for the previous reason.

If we let $a = 0$, the equations(30)-(31) give the results of the Schwarzschild black hole[20]. In the following steps, we will use the equations(30)-(31) to evaluate the quasinormal mode frequencies when $a \neq 2M$.

From Fig.2, we know that the effective potential V , which depends only on the value of r for fixed $|\kappa|$ and a , has a maximum over $r \in (2M, +\infty)$. The location r_0 of the maximum has to be found numerically. But for $|\kappa| \rightarrow \infty$, we can get the position of the potential peak from $V_{1,2}$,

$$r_0 (|\kappa| \rightarrow \infty) \rightarrow \frac{a + 6M}{4} \left(1 + \sqrt{1 - \frac{32aM}{(a + 6M)^2}} \right), \quad (32)$$

and

$$\begin{aligned} r_0 (|\kappa|) &\leq r_0 (|\kappa| \rightarrow \infty) && (\text{for } V_1), \\ r_0 (|\kappa|) &\geq r_0 (|\kappa| \rightarrow \infty) && (\text{for } V_2). \end{aligned}$$

If we treat the mass M of the black hole as a unit of mass and length, the value of the r_0 ($|\kappa| \rightarrow \infty$) only depends on the coupling coefficient a . It gives $r_0(|\kappa| \rightarrow \infty) = 3$ for a black hole with $a = 0$, which agrees with the result for the Schwarzschild black hole[20]. From Fig.3, we see that the peak value of the effective potential V increases with a .

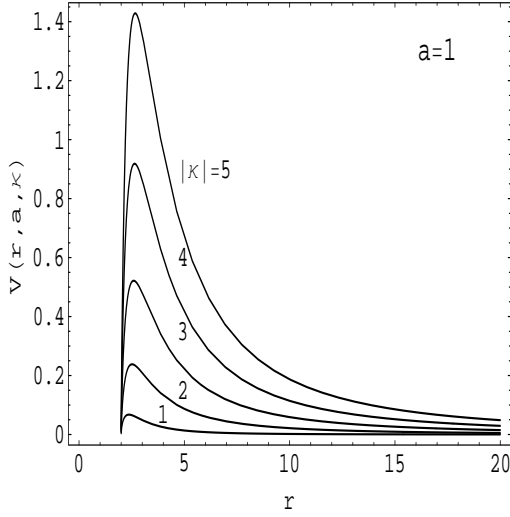


Figure 2: Variation of the effective potential V for massless Dirac field V with κ as $a = 1$.

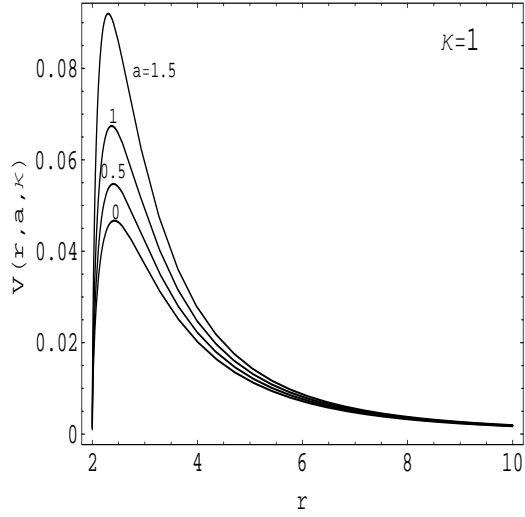


Figure 3: Variation of the effective potential V for massless Dirac field with a as $\kappa = 1$.

1 Dirac quasinormal mode frequencies by using WKB approximation

We now evaluate the quasinormal mode frequencies for the massless Dirac field in Garfinkle-Horowitz-Strominger black hole using the WKB potential approximation. In Sec.II, we have used this kind of approximation to evaluate the quasinormal mode frequencies for scalar field. We just need plug the effective potential $V(r, a, k)$ in Eq.(31) into Eq.(17) and use Eqs.(13)-(16) to evaluate the complex frequencies for Dirac field. Here we only list the results for positive n in Table V, the corresponding values for positive κ are plotted in Fig.8.

2 Dirac quasinormal mode frequencies by using Pöschl-Teller approximation

The potential $V_{1,2}$ calculated by Eq.(29) are smooth function, integrable over the range of $r_* \in (-\infty, +\infty)$, i.e.,

$$\begin{aligned} V &\rightarrow e^{\frac{r_*}{2M}}, & \text{as } r_* &\rightarrow -\infty, \\ V &\rightarrow r_*^{-2}, & \text{as } r_* &\rightarrow +\infty. \end{aligned}$$

From this relation, we know that the effective potential drops exponentially to zero as $r_* \rightarrow -\infty$ (but falls off as r_*^{-2} as $r_* \rightarrow +\infty$). So we can study the Dirac quasinormal modes by using the Pöschl-Teller approximation potential, [17, 23]

$$V_{PT} = \frac{V_0}{\cosh^2 \alpha(r_* - r_0)}. \quad (33)$$

The quantities V_0 and $\alpha > 0$ are given by the height and curvature of the potential at its maximum ($r_* = r_0$), i.e.,

$$V_0 = V(r_0), \quad \alpha^2 = -\frac{1}{2V_0} \left[\frac{d^2V}{dr_*^2} \right]_{r_0}. \quad (34)$$

The quasinormal mode frequencies of the Pöschl-Teller potential can be evaluated analytically[23]

$$\omega_n = \sqrt{V_0 - \frac{\alpha^2}{4}} - \alpha(n + 1/2)i, \quad (n = 0, 1, 2, \dots). \quad (35)$$

The results for positive n are listed in Table VI. From Table V and Table VI, we see that the values evaluated by this two kinds of approximation have a good agreement with each other. The real part of the complex frequencies, which decreases slowly as mode number n increases, keeps unchanged as n changes as showed in Fig.8. However, as to the magnitude of the imaginary part of the frequencies evaluated by these two kinds of approximations, both increase with n . Therefore, both approximations will break down when n is large. In this article, we see that the accuracy of two methods is good enough for any $n < \kappa$. It is also showed in Fig.8 that the complex frequencies increases with a . This indicates that the QNMs with higher dilaton decay more rapidly.

B Quasinormal mode frequencies for the massive Dirac field

In this subsection, we shall evaluate the quasinormal mode frequencies of the massive Dirac field as $a \neq 2M$ in the Garfinkle-Horowitz-Strominger black hole by using Pöschl-Teller potential approximation.

We can rewrite Eq.(27) as

$$\frac{d^2\tilde{F}}{d\tilde{r}_*^2} + (\omega^2 - V)\tilde{F} = 0, \quad (36)$$

where

$$\tilde{r}_* = r + 2 \ln(r/2 - 1) + \frac{1}{2\omega} \tan^{-1} \left(m\sqrt{r(r-a)}/\kappa \right), \quad (37)$$

$$\begin{aligned} V = & \frac{e^{2U} (\kappa^2 + m^2 R^2)^{3/2}}{R^2 [(\kappa^2 + m^2 R^2) + e^{2U} m\kappa R'/2\omega]^2} \cdot \{ e^U U' R (\kappa^2 + m^2 R^2) \\ & - \kappa^2 e^U R' - \frac{1}{2\omega} \frac{e^{3U} \kappa m R}{(\kappa^2 + m^2 R^2) + e^{2U} \kappa m R'/2\omega} [(\kappa^2 + m^2 R^2) \\ & \cdot (2U' R' + R'') - 2m^2 R R'^2] + (\kappa^2 + m^2 R^2)^{3/2} \}. \end{aligned} \quad (38)$$

The dependence of potential $V(r, m, \kappa, a, \omega)$ on m , κ , a and ω is showed in Fig.(4-7), respectively. From Fig.4, we can see that the peak of the potential increases with m . However, the potential has an asymptotic value m^2 as $r \rightarrow \infty$. Hence, there exists a maximum m_{max} above which the height of the peak is lower than the asymptotic value m^2 . As a result, there will be no quasinormal modes when m is larger than m_{max} . So we can use the same method which we have used in Sec.II to estimate this maximum value.

$$V(r_{max}, m_{max}, \kappa, a, \omega = m_{max}) = (m_{max})^2. \quad (39)$$

The values calculated in this way are tabulated in Table III and Table IV, where we have also given the maximum values of $\mu = m/\kappa$ which will be used in the following discussions.

Fig.5 shows the dependence of the potential on the angular momentum quantum number κ , from which we see that the behaviors of the potential in this case are similar to that of the massless one as showed in Fig.2. The same case happens in the relation between potential V and a , as showed in Fig.3 and Fig.6. The variation of the potential with a for massive Dirac field approaches to that of massless one. However, Fig.7 shows that the potential for massive Dirac field depends obviously on the energy

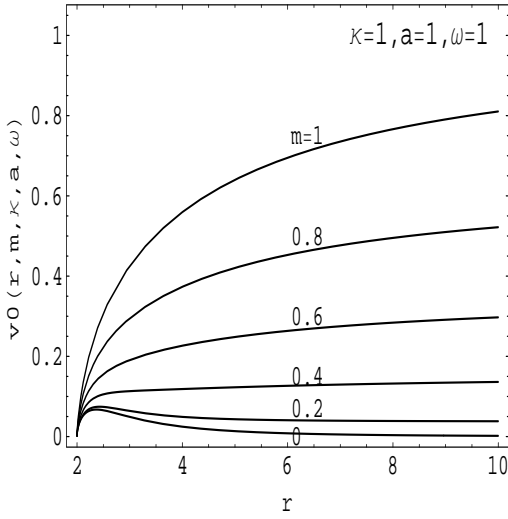


Figure 4: Variation of the effective potential V for massive Dirac field with m as $\kappa = 1, a = 1, \omega = 1$.

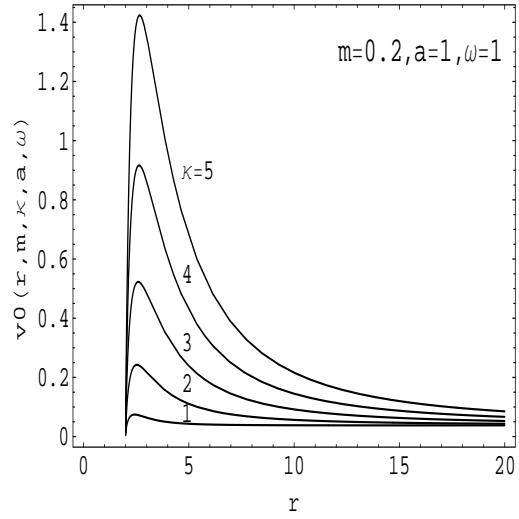


Figure 5: Variation of the effective potential V for massive Dirac field with κ as $m = 0.2, a = 1, \omega = 1$.

(or frequency) ω . This tells us that we can't evaluate the quasinormal mode frequencies as done for the massless ones. In the following parts, we'll evaluate the complex quasinormal mode frequencies for massive Dirac field by using Pöschl-Teller potential approximation.

From Table III and IV, we can see that $|\mu_{max}| < 1$ for any $\kappa \neq 0$, and as $|\kappa| \rightarrow \infty, \mu \rightarrow 0$ regardless of the value of m . Therefore, we can evaluate the quasinormal mode frequencies in the Pöschl-Teller approximation as power series of μ for given values of κ as showed in [20, 24, 25]. The position r_{max} of the peak of the massive potential can be obtained by expanding r as power series of μ up to order μ^6 ,

$$r_{max} = r_0 + r_1\mu + r_2\mu^2 + r_3\mu^3 + r_4\mu^4 + r_5\mu^5 + r_6\mu^6 = r_0 + \Sigma, \quad (40)$$

and requires

$$0 = V'(r_{max}) = V'(r_0) + \Sigma V''(r_0) + \frac{1}{2}\Sigma^2 V'''(r_0) + \frac{1}{6}\Sigma^3 V^{(4)}(r_0) + \frac{1}{24}\Sigma^4 V^{(5)}(r_0) + \frac{1}{120}\Sigma^5 V^{(6)}(r_0) + \frac{1}{720}\Sigma^6 V^{(7)}(r_0), \quad (41)$$

where r_0 is the position of the peak value for the massless case obtained in the last section. The coefficients r_i can be then evaluated order by order from this equation. In the following step, we expand ω up to order μ^6

$$\omega = \omega_0 + \omega_1\mu + \omega_2\mu^2 + \omega_3\mu^3 + \omega_4\mu^4 + \omega_5\mu^5 + \omega_6\mu^6, \quad (42)$$

and plug it into r_{max} , then expand it again up to order μ^6 . Using this new expansion for r_{max} , we can expand the right hand side of Eq.(35). Note that Eq.(34) should be written as

$$V_0 = V(r_{max}), \quad \alpha^2 = -\frac{1}{2V_0} \left[\frac{d^2V}{d\tilde{r}_*^2} \right]_{r_{max}}. \quad (43)$$

Then we can solve ω_i self-consistently order by order in μ . The values evaluated in this way are listed in Tables(VII-VIII). Quasinormal mode frequencies for any fixed $\mu < \mu_{max}$ can be obtained by plugging these coefficients into Eq.(42). Fig.9 is the corresponding figure, from which, we can see that the real parts of the quasinormal mode frequencies increase with m , but the magnitude of the imaginary parts of the frequencies decrease as m increase. This means that field with higher mass will decay more slowly.

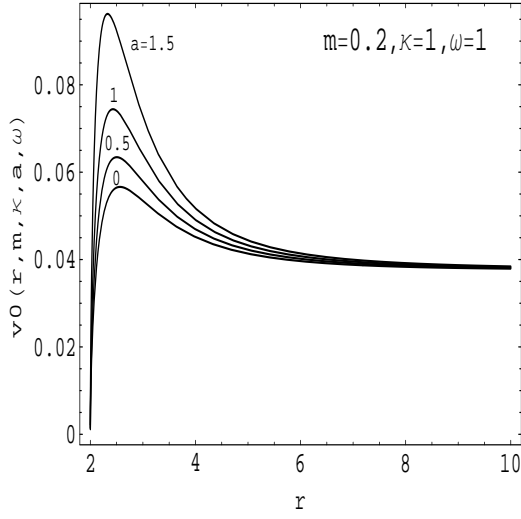


Figure 6: Variation of the effective potential V for massive Dirac field with a as $m = 0.2, \kappa = 1, \omega = 1$.

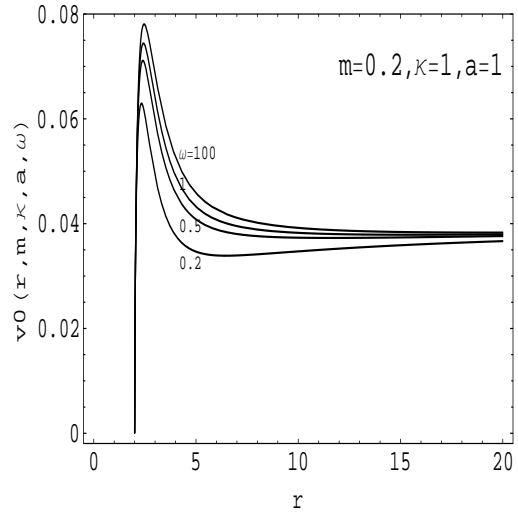


Figure 7: Variation of the effective potential V for massive Dirac field with ω as $m = 0.2, \kappa = 1, a = 1$.

κ	$a = 0$		$a = 0.5$		$a = 1$	
	m	μ	m	μ	m	μ
1	0.2245	0.2245	0.2414	0.2414	0.2652	0.2652
2	0.4527	0.2263	0.4888	0.2444	0.5392	0.2696
3	0.6963	0.2321	0.7505	0.2502	0.8263	0.2754
4	0.9436	0.2359	1.0158	0.2539	1.1165	0.2791
5	1.1922	0.2384	1.2823	0.2565	1.4080	0.2816

Table III: Maximum values of the mass m and $\mu(= m/\kappa)$ of the Dirac field above which QNMs can't occur for positive κ .

κ	$a = 0$		$a = 0.5$		$a = 1$	
	m	μ	m	μ	m	μ
1	0.3333	-0.3333	0.3524	-0.3524	0.3780	-0.3780
2	0.5723	-0.2862	0.6089	-0.3045	0.6589	-0.3295
3	0.8190	-0.2730	0.8732	-0.2911	0.9479	-0.3160
4	1.0673	-0.2668	1.1394	-0.2849	1.2389	-0.3097
5	1.3164	-0.2633	1.4063	-0.2813	1.5306	-0.3061

Table IV: Maximum values of the mass m and $\mu(= m/\kappa)$ of the Dirac field above which QNMs can't occur for negative κ .

IV SUMMARIES AND DISCUSSIONS

Both scalar and Dirac quasinormal mode frequencies in Garfinkle-Horowitz-Strominger black hole are evaluated by using WKB approximation and Pöschl-Teller approximation. As for scalar field, the complex frequencies depend on the mass m of the field, the orbital angular momentum l , and the coupling coefficient a . From the results we have obtained in Table II and Fig.1, we can see that the real parts of the frequencies increase with m and a , but they decrease with n . However, the magnitude of the imaginary parts of the frequencies increase with a and n , but decrease with m . This indicates that field with higher mass will decay more slowly, while QNMs with higher dilaton will decay more rapidly. The similar behaviors appear in the Dirac field. But for massive Dirac cases, we have made an expansion in powers of the parameter $\mu = m/\kappa$. In this way, we can obtain the numerical values of the quasinormal mode frequencies.

Another conclusion is that the quasinormal mode frequencies evaluated by using WKB approximation agree with the results obtained by using Pöschl-Teller approximation when mode number n is small, as showed in Fig.8. It is important that we have the same conclusion for massive cases.

ACKNOWLEDGEMENTES

One of the authors(Fu-Wen Shu) wish to thank Doctor Xiang Li, Jia-Feng Chang and Xian-Hui Ge for their valuable discussions. The work was supported by the National Natural Science Foundation of China under Grant No. 10273017.

Table V: Dirac quasinormal mode frequencies by using WKB approximation

κ	n	$a = 0$	$a = 0.5$	$a = 1$	$a = 1.5$
1	0	0.1765-0.1001i	0.1976-0.1025i	0.2275-0.1054i	0.2780-0.1083i
2	0	0.3786-0.0965i	0.4168-0.0994i	0.4716-0.1028i	0.5651-0.1061i
	1	0.3536-0.2988i	0.3947-0.3061i	0.4534-0.3147i	0.5536-0.3226i
5	0	0.9602-0.0963i	1.0539-0.0992i	1.1889-0.1025i	1.4192-0.1058i
	1	0.9496-0.2902i	1.0445-0.2987i	1.1810-0.3088i	1.4137-0.3180i
	2	0.9300-0.4876i	1.0269-0.5015i	1.1661-0.5175i	1.4037-0.5323i
	3	0.9036-0.6892i	1.0032-0.7081i	1.1460-0.7297i	1.3902-0.7493i
	4	0.8721-0.8944i	0.9749-0.9180i	1.1222-0.9451i	1.3744-0.9690i

Table VI: Dirac quasinormal mode frequencies by using Pöschl-Teller approximation

κ	n	$a = 0$	$a = 0.5$	$a = 1$	$a = 1.5$
1	0	0.1890-0.1048i	0.2083-0.1064i	0.2360-0.1082i	0.2829-0.1092i
2	0	0.3855-0.0991i	0.4229-0.1015i	0.4766-0.1043i	0.5684-0.1068i
	1	0.3855-0.2972i	0.4229-0.3045i	0.4766-0.3130i	0.5684-0.3203i
5	0	0.9625-0.0966i	1.0561-0.0995i	1.1908-0.1028i	1.4204-0.1059i
	1	0.9625-0.2899i	1.0561-0.2984i	1.1908-0.3084i	1.4204-0.3176i
	2	0.9625-0.4832i	1.0561-0.4974i	1.1908-0.5140i	1.4204-0.5293i
	3	0.9625-0.6764i	1.0561-0.6964i	1.1908-0.7195i	1.4204-0.7411i
	4	0.9625-0.8697i	1.0561-0.8953i	1.1908-0.9251i	1.4204-0.9528i

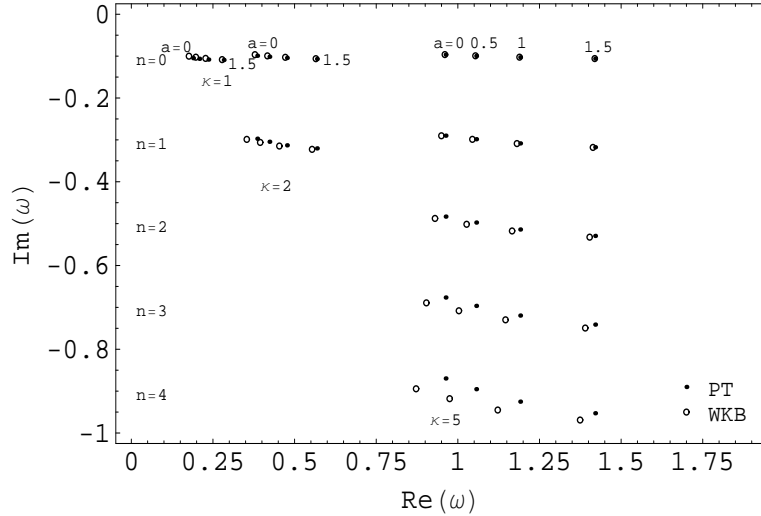


Figure 8: Massless Dirac quasinormal mode frequencies evaluated by using WKB and Pöschl-Teller potential approximation

Table VII: The real parts of the quasinormal mode frequencies for massive Dirac field

a	κ	n	ω_0	ω_1	ω_2	ω_3	ω_4	ω_5	ω_6		
0	1	0	0.1890	-0.1306	1.1736	-1.2880	-1.2438	25.707	-104.57		
		2	0.3855	-0.1583	1.8235	0.3132	-0.1220	2.0807	4.3001		
	5	1	0.3855	-0.1207	1.8048	-0.4484	2.3177	-4.2165	-8.5152		
		0	0.9625	-0.1654	4.3544	0.4607	2.6316	1.8376	14.149		
		1	0.9625	-0.1572	4.3535	0.2019	2.9479	2.7027	6.5863		
		2	0.9625	-0.1439	4.3510	-0.1557	3.4228	1.9923	-0.4496		
		3	0.9625	-0.1294	4.3472	-0.4621	3.8330	-1.0875	-0.8916		
		4	0.9625	-0.1160	4.3433	-0.6652	4.0637	-5.3255	3.8645		
		0.5	1	0	0.2083	-0.1350	0.9330	0.0801	-0.2485	-1.0873	-0.3100
				2	0.4229	-0.1497	1.5490	0.1968	0.2509	1.2826	2.5888
5	1		0.4229	-0.1166	1.5328	-0.3105	1.8138	-2.5407	-2.8215		
	0		1.0561	-0.1555	3.7113	0.2922	2.3756	1.1681	9.1466		
	1		1.0561	-0.1484	3.7104	0.1269	2.5702	1.4507	5.7704		
	2		1.0561	-0.1368	3.7083	-0.1086	2.8675	0.9400	2.4967		
	3		1.0561	-0.1236	3.7051	-0.3182	3.1369	-0.7745	2.1499		
	4		1.0561	-0.1111	3.7017	-0.4620	3.3019	-3.1439	4.3852		
	1		1	0	0.2360	-0.1265	0.7241	0.0224	0.0763	-0.4976	0.5058
				2	0.4766	-0.1385	1.2327	0.0933	0.4391	0.6423	1.5177
5		1	0.4766	-0.1110	1.2196	-0.1944	1.2855	-1.3001	0.1945		
		0	1.1908	-0.1430	2.9092	0.1280	3.0462	1.0794	-3.0867		
		1	1.1908	-0.1439	2.8908	-0.1161	3.3237	4.6232	-2.5366		
		2	1.1908	-0.1452	2.8650	-0.5293	3.5692	9.5014	-0.0203		
		3	1.1908	-0.1468	2.8439	-1.0123	3.5679	13.628	3.5289		
		4	1.1908	-0.1484	2.8326	-1.4886	3.3481	16.245	6.0940		

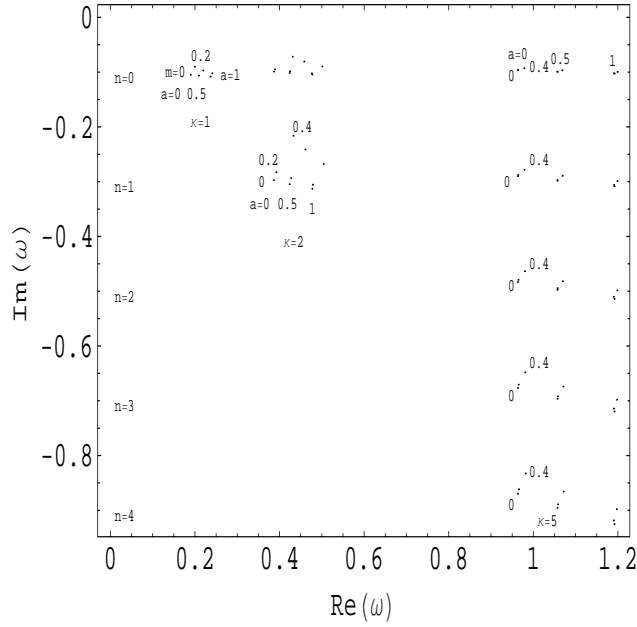


Figure 9: Massive Dirac quasinormal mode frequencies

Table VIII: The imaginary parts of the quasinormal mode frequencies for massive Dirac field

a	κ	n	ω_0	ω_1	ω_2	ω_3	ω_4	ω_5	ω_6	
0	1	0	-0.1048	-0.0629	0.4857	0.7429	-3.6364	15.433	41.564	
		2	-0.0991	-0.0292	0.6419	0.5097	0.4961	3.9247	18.790	
	2	1	-0.2972	-0.0586	1.9232	0.6183	4.1854	12.488	3.3177	
		5	0	-0.0966	-0.0112	0.7081	0.2414	1.0021	1.0909	9.5112
		1	-0.2899	-0.0310	2.1245	0.6171	3.1196	4.5254	23.934	
	3	2	-0.4832	-0.0450	3.5407	0.7701	5.5208	9.4815	29.923	
		3	-0.6764	-0.0528	4.9555	0.7419	8.2001	13.885	32.585	
		4	-0.8697	-0.0559	6.3684	0.6276	11.014	16.435	37.898	
		5	0	-0.1064	-0.0555	0.4235	0.4624	-1.1012	5.0715	0.3089
	0.5	1	0	-0.1015	-0.0262	0.5267	0.3303	0.5246	2.5273	9.7331
1			-0.3045	-0.0547	1.5759	0.4160	3.2193	7.3289	5.7093	
5		0	-0.0995	-0.0101	0.5766	0.1567	0.9083	0.7544	6.2479	
		1	-0.2984	-0.0284	1.7298	0.4049	2.7927	2.8027	16.737	
		2	-0.4974	-0.0418	2.8828	0.5128	4.8468	5.5232	23.440	
		3	-0.6964	-0.0498	4.0346	0.4989	7.0743	7.9666	28.421	
1	1	0	-0.1082	-0.0468	0.3346	0.2387	-0.4409	2.8934	-1.6048	
		2	-0.1043	-0.0225	0.4041	0.1797	0.4793	1.3415	4.2433	
		1	-0.3130	-0.0495	1.2077	0.2342	2.2696	3.5442	5.2856	
		5	0	-0.1028	0.0012	0.4498	0.3779	0.7181	-3.0411	2.0343
	2	1	-0.3084	0.0035	1.3419	1.0698	2.3336	-7.6403	5.5251	
		2	-0.5140	0.0053	2.2172	1.6034	4.2615	-9.1513	9.3059	
		3	-0.7195	0.0065	3.0780	1.9521	6.3210	-8.1271	15.282	
		4	-0.9251	0.0071	3.9316	2.1405	8.3013	-5.8811	23.284	

References

- [1] T.Regge, and J.A.Wheeler, *Phys.Rev.* **108**,1064(1957).
- [2] D.R.Brill, and J.A.Wheeler, *Rev.Mod.Phys.* **29**,465(1957).
- [3] C.V.Vishveshwara, *Nature*, **227**,936(1970).
- [4] S.Chandrasekhar, and S.Detweller, *Proc.R.Soc.Lond.A* **344**, 441(1975).
- [5] S.Chandrasekhar, *The Mathematical Theory of Black Holes*(Oxford University Press,Oxford,England,1983).
- [6] V.P.Frolov, and I.D.Novikov, *Black Hole Physics:Basic Concepts and New Developments* (Kluwer Academic publishers,1998).
- [7] S.Hod, *Phys. Rev. Lett.* **81**, 4293(1998).
- [8] O.Dreyer, *Phys. Rev. Lett.* **90**, 081301(2003).
- [9] A.Corichi, *Phys.Rev.D* **67**, 087502(2003).
- [10] J.Maldacena, *Adv.Theor.Math.Phys.* **2**, 231(1998)
- [11] S.Kalyana Rama and B.Sathiapalan, *Mod.Phys.Lett.A* **14**, 2635(1999).
- [12] G.Gibbons and K.Maeda, *Nucl.Phys.* **B298**, 741(1988).
- [13] D.Garfinkle, G.T.Horowitz, and A.Strominger, *Phys.Rev.D* **43**, 3140(1991).

- [14] J.L.Jing, *Phys.Rev.D* **69**, 084009(2004)..
- [15] B.F.Schutz, and C.M.Will, *Astrophys.J.Lett.Ed.* **291**, L33(1985).
- [16] S.Iyer and C.M.Will, *Phys.Rev.D* **35**, 3621(1987).
- [17] G.Pöschl and E.Teller, *Z.Phys.***83**, 143(1933).
- [18] S.Iyer, *Phys.Rev.D***35**, 3632(1987).
- [19] A.Ghosh and P.Mitra, *Phys. Rev. Lett.* **73**, 2521(1994).
- [20] H.T.Cho, *Phys.Rev.D* **68**, 024003(2003).
- [21] A.Anderson and R.H.Price, *Phys.Rev.D* **43**, 3147(1991).
- [22] A.Zhidenko, *Class.Quant.Grav.* **21**, 273(2004).
- [23] V.Ferrari and B.Mashhoon, *Phys.Rev.D* **30**, 295(1984).
- [24] E.Seidel and S.Iyer, *Phys.Rev.D* **41**, 374(1990).
- [25] L.E.Simone and C.M.Will, *Class.Quant.Grav.* **9**, 963(1992).